CFS CANADIAN FOREST SERVICE

A procedure for mapping and monitoring mountain pine beetle red attack forest damage using landsat imagery

M.A. Wulder, J.C. White, N.C. Coops, T. Han, M.F. Alvarez, C.R. Butson, and X. Yuan

Natural Resources Canada • Canadian Forest Service
Pacific Forestry Centre • Victoria, British Columbia
Information Report • BC-X-404

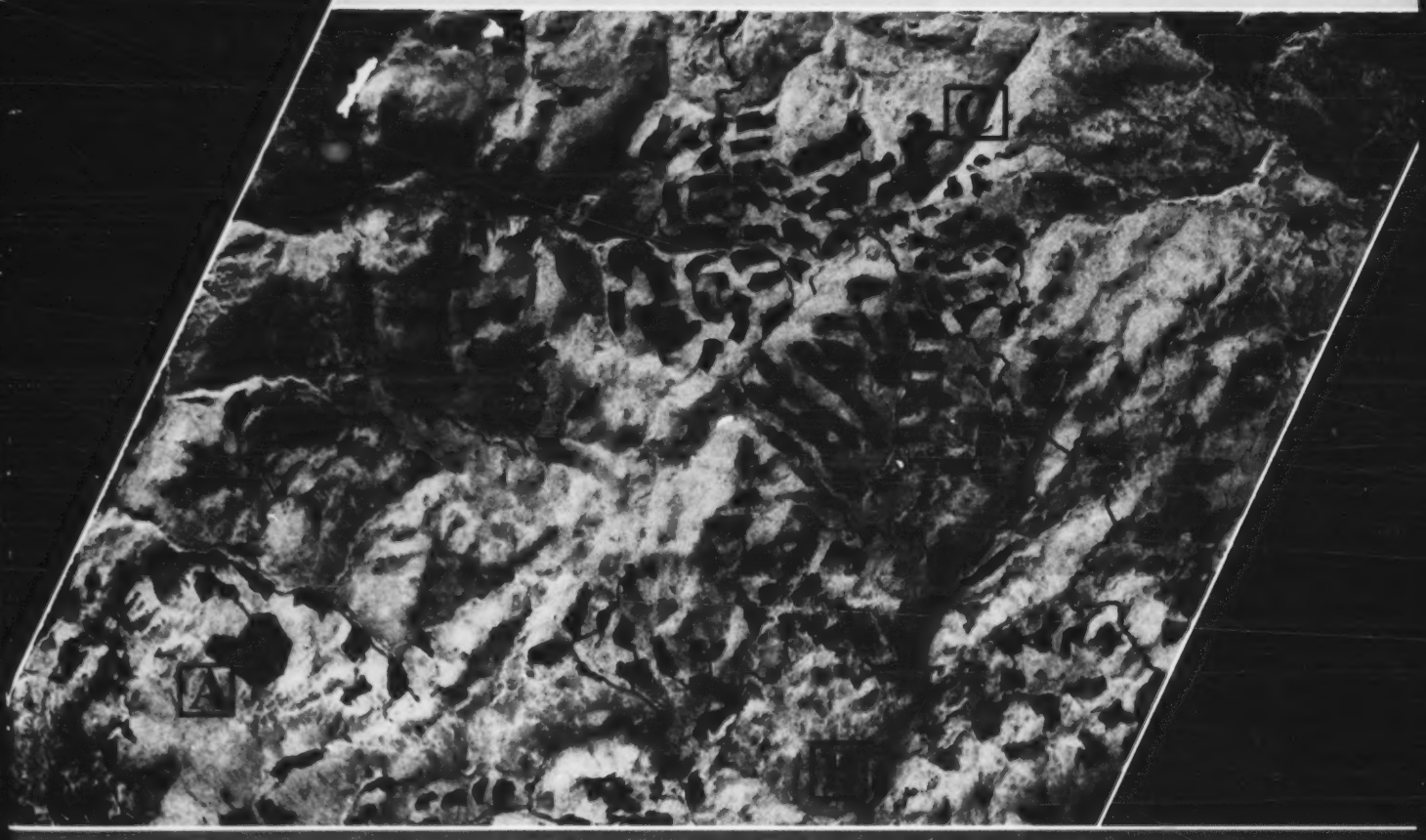

Natural Resources Canada | Ressources naturelles Canada

Canada

The Pacific Forestry Centre, Victoria, British Columbia

The Pacific Forestry Centre of the Canadian Forest Service undertakes research as part of a national network system responding to the needs of various forest resource managers. The results of this research are distributed in the form of scientific and technical reports and other publications.

Additional information on Natural Resources Canada, the Canadian Forest Service, and Pacific Forestry Centre research and publications is also available on the World Wide Web at: **www.pfc.cfs.nrcan.gc.ca.** To download or order additional copies of this publication, see our online bookstore at: **bookstore.cfs.nrcan.gc.ca.**

2008-04975/

A procedure for mapping and monitoring mountain pine beetle red attack forest damage using landsat imagery

M.A. Wulder[1*], J.C. White[1], N.C. Coops[2],
T. Han[1], M.F. Alvarez[3], C.R. Butson[1], and X. Yuan[4]

[1]Canadian Forest Service, Pacific Forestry Centre,
506 West Burnside Road, Victoria, British Columbia, V8Z 1M5, Canada

[2]Department of Forest Resource Management, 2424 Main Mall, University of British Columbia,
Vancouver, British Columbia, V6T 1Z4, Canada

[3] Universidad de León, E.S.T. Ingeniería de Minas, Avd. Astorga s/n 24400,
Ponferrada, Leon, Spain

[4] British Columbia Ministry of Forests and Range, Forest Analysis and Inventory Branch,
395 Waterfront Crescent, Victoria, British Columbia, V8T 5K7, Canada

*Corresponding Author
Phone: (250) 363-6090;
Fax: (250) 363-0775;
Email: mwulder@nrcan.gc.ca

Natural Resources Canada
Canadian Forest Service
Pacific Forestry Centre
Information Report BC-X-404

2006

Canadian Forest Service
Pacific Forestry Centre
506 West Burnside Road
Victoria, British Columbia
V8Z 1M5
Phone (250) 363-0600

www.pfc.cfs.nrcan.gc.ca

© Her Majesty the Queen in Right of Canada, 2006

ISSN 0830-0453
ISBN 0-662-43290-8
Printed in Canada

Microfiches of this publication may be purchased from:
MicroMedia Inc.
240 Catherine Street, Suite 305
Ottawa, ON K2P 2G8

Library and Archives Canada Cataloguing in Publication

A procedure for mapping and monitoring mountain pine beetle red attack
forest damage using Landsat imagery / M.A. Wulder ... [et al.].

(Information report ; BC-X-404)
Includes bibliographical references.
Includes summary in French.
ISBN 0-662-43290-8
Cat. no.: Fo143-2/404E

1. Mountain pine beetle--Monitoring--British Columbia. 2. Lodgepole
pine--Diseases and pests--British Columbia--Remote sensing. 3. Lodgepole pine--
Diseases and pests--Remote sensing--Methodology. 4. Artificial satellites in forestry.
5. Forest mapping--Methodology. 6. LANDSAT satellites. I. Wulder, Michael A.
(Michael Albert), 1968- II. Pacific Forestry Centre III. Title. IV. Series: Information report (Pacific Forestry
Centre) ; BC-X-404

SB945.M78P76 2006 634.9'7516768 C2006-980110-X

Contents

Abstract / Résumé v
1.0 Background information 1
1.1 Mountain pine beetle life cycle 1
1.2 Mapping mountain pine beetle 2
1.3 The advantages of a data hierarchy 2
1.4 Logistical issues to the mapping procedure 3
2.0 Enhanced Wetness Difference Index (EWDI) approach to mapping red attack 5
3.0 Methodology 5
3.1 Required data 7
3.2 Scene selection 8
3.3 Ancillary data preprocessing 9
3.4 Image preprocessing 10
3.4.1 Assess quality/suitability of imagery 10
3.4.2 Geometric correction 11
3.4.3 Conversion from TM to ETM+ 11
3.4.4 Radiometric correction 12
3.5 Image Normalization 15
3.6 Enhanced Wetness Difference Index 16
3.6.1 Tasselled Cap Transformation (TCT) 16
3.6.2 Wetness differencing 17
3.6.3 Enhanced Wetness Difference Index (EWDI) visual display 17
3.6.4 Threshold determination 18
3.7 Accuracy assessment 19
3.8 Level of effort 22
4.0 Recommendations 23
5.0 Conclusions 26
6.0 Acknowledgements 27
7.0 References 28

List of Tables

Table 1. Image selection criteria based on year and month combinations for mapping red attack. 8
Table 2. A summary of masks used for vetting calibration and validation data and for restricting image analysis and product output. 10
Table 3. Coefficients for conversion of Landsat TM to ETM+ equivalent....12
Table 4. Earth-Sun distance in astronomical unit (Source: Huang et al. 2002b)....14
Table 5. ETM+ Mean solar exoatmospheric irradiances (Source: Huang et al. 2002b). 14
Table 6. TCT transformation coefficients for ETM+ TOA data. 17
Table 7. Example of error (confusion) matrix for a hypothetical mountain pine beetle detection study with two classes....19
Table 8. Classification accuracies of the EWDI procedure for three test sites. 21
Table 9. Estimated amount of effort associated with each of the tasks required to implement the protocol outlined in this report....22

List of Figures

Figure 1. Summary of steps included in the processing flow to generate a map of mountain pine beetle red attack damage from two dates of Landsat TM/ETM+ imagery. 6
Figure 2. Required data checklist for red attack mapping of mountain pine beetle....7
Figure 3. Illustration of the cloud mask, ...15
Figure 4. A sample of the EWDI from southern British Columbia. 18
Figure 5. Generalized distributions capturing the EWDI values representative of red attack pixels and non-attack pixels. 19
Figure 6. Location of test sites in British Columbia, Canada. 21

Abstract

Remote sensing is a useful technology for detecting and mapping the red attack stage of a mountain pine beetle infestation. Provided appropriate imagery is selected to coincide with the manifestation of the red attack damage, the damage can be mapped in an accurate and timely fashion using Landsat Thematic Mapper or Enhanced Thematic Mapper Plus imagery and change detection methods. This report describes a detailed procedure for using multiple dates of Landsat imagery to generate information products indicating the location and extent of mountain pine beetle red attack damage. The accuracy of this procedure is assessed and reported using more detailed forest health survey information at three sites in British Columbia. Also documented in this report is an optimal approach for Landsat scene selection, a summary of the level of effort required to apply the procedure described herein, and recommendations for potential improvements to the mapping procedure. Details on data acquisition, image pre-processing, image analysis, and accuracy assessment are included to facilitate the implementation for the mapping procedure in an operational context.

Résumé

La télédétection s'avère une technique utile pour détecter et cartographier une infestation de dendroctones du pin ponderosa au stade rouge. À condition que l'imagerie appropriée soit sélectionnée pour correspondre aux signes des dommages causés au stade rouge, on peut cartographier ces derniers de manière précise et au bon moment en recourant à l'imagerie des capteurs Landsat TM ou TM amélioré (ETM+) et en modifiant les méthodes de détection. Le présent rapport décrit dans le détail comment utiliser des images Landsat TM prises à des dates différentes pour générer des produits d'information qui indiqueront l'emplacement et l'étendue des dommages causés par le dendroctone du pin ponderosa au stade rouge d'infestation. La précision de la procédure est évaluée et constatée au moyen de renseignements plus détaillés provenant d'une enquête sur la santé de la forêt effectuée à trois endroits en Colombie-Britannique. Le rapport traite également de la meilleure approche pour sélectionner des vues Landsat. On y trouve aussi un résumé de ce qu'il faut faire pour mettre en application la procédure de cartographie décrite et des recommandations au sujet d'éventuelles améliorations à y apporter. Des détails sur l'acquisition des données, le prétraitement des images, l'analyse des images et l'évaluation de la précision sont fournis afin de faciliter la mise en œuvre de la procédure de cartographie dans un contexte d'exploitation.

1.0 Background information

In western Canada, the mountain pine beetle (*Dendroctonus ponderosae* Hopkins) population has reached epidemic levels, primarily in British Columbia, with the area of infested forest increasing from approximately 164,000 ha in 1999 to 8.5 million hectares in 2005 (British Columbia Ministry of Forests and Range, 2006). At epidemic population levels, mountain pine beetles generally spread through mature stands and cause extensive mortality of large-diameter trees. Even though virtually all species of pine within the mountain pine beetle's range are suitable hosts (Furniss and Schenk, 1969; Smith et al. 1981), lodgepole pine (*Pinus contorta* Dougl. ex Loud. var. *latifolia* Engelm.) is considered the beetle's primary host, due to the trees' size and relative abundance across the Pacific Northwest.

The biological range of lodgepole pine exceeds the current range of the mountain pine beetle. Recent research has indicated that the beetle is expanding into new geographic areas (Carroll et al. 2004). The two main factors that have contributed to the successful expansion of the beetle population in British Columbia include the large amount of mature lodgepole pine on the land base, which has tripled in the last century as a result of intensive fire suppression activities (Taylor and Carroll 2004) and several successive years of favourable climatic conditions (i.e., warmer than average winters), resulting in an increase in climatically suitable areas for brood development (Carroll et al. 2004).

1.1 Mountain pine beetle life cycle

In general, mountain pine beetles in British Columbia produce a single generation per year (Safranyik et al. 1974; Carroll and Safranyik 2004). Adult beetles typically attack trees between mid-July and mid-August and lay eggs, completing their development cycle into mature adults approximately one year later (Amman and Cole, 1983).

The mountain pine beetle uses two tactics to overcome the defences of a susceptible tree. First, beetles may attack in large numbers through a cooperative behaviour termed "mass attack". By rapidly concentrating their attack on selected trees, the beetles are capable of exhausting the host's defensive response (Safranyik et al. 1974; Berryman et al. 1989). Secondly, the beetles have a close association with several microorganisms that the beetles carry into the tree with them when they attack. In particular, the spores of two blue stain fungi (*Ophiostoma clavigerum* and *Ophiostoma montium*) are inoculated into the tree as the beetles bore through the bark. These fungal spores penetrate living cells in the phloem and xylem (Safranyik et al. 1975; Ballard et al. 1982, 1984; Solheim 1995), resulting in desiccation and disruption of transpiration (Mathre 1964), effectively stopping resin production by the tree (Carroll and Safranyik 2004).

Immediately following a mass attack, the foliage of trees remains visibly unchanged; however, a drop in sapwood moisture has been measured as a consequence of the attack (Reid 1961; Yamaoka et al. 1990). When the host tree is killed, but still has green foliage, it is in the green attack stage. The first visible sign of impact is a change in foliage colour from green to greenish-yellow that usually begins in the top of the crown. These trees are referred to as faders. Generally, the foliage fades from green to yellow to red over the spring and summer following a previous year of attack (Amman 1982; Henigman et al. 1999). The leaves gradually desiccate and the pigment molecules break down; initially the green chlorophyll pigment molecules are lost, then the yellow carotenes and red anthocyanins (Hill et al. 1967). Slowly, the needles drop until the tree is completely defoliated. Twelve months after being attacked, over 90% of the killed trees will have red needles (red attack). Three years after being attacked, most trees will have lost all needles (grey attack) (British Columbia Ministry of Forests 1995). There is variability associated with the progression of attack stages as the rate at which the foliage will discolour varies by species and by site (Safranyik 2004).

1.2 Mapping mountain pine beetle

Information regarding the location, size, and impact of mountain pine beetle populations is collected using a variety of survey techniques. The survey method used is selected based on the information required for a particular aspect of forest management. The survey may be done on a tree-by-tree basis on the ground, from an airborne platform, or using satellite-based sensors. As a result, the extent of the survey may range from a few hectares to millions of hectares. Each survey method has limitations, with the collected data being applicable to different management situations (Wulder et al. 2005a). Also, each level of this data hierarchy satisfies the specific information requirements of forest inventory, modelling, and planning. A summary of existing methods of survey and their associated costs are described in the detailed review in Wulder et al. (2004a).

Aerial overview surveys are often the most appropriate techniques for large area surveying of mountain pine beetle damage due to the inherent speed and efficiency with which they can be completed. The general approach to detection is to sketch map the red trees that are visible from a fixed wing aircraft on to topographic maps at scales from 1:100 000 to 1:250 000. The aerial overview surveys may be conducted on an annual basis to provide sufficient information to characterize the general location of the damage, to approximate the gross area of damage, and to indicate the general trend in damage from one year to the next. However, the shortcomings of these overview surveys (which include large errors of omission when damage is very light), subjectivity in boundary delineations, and the variability in estimates of attack magnitude, limit the utility of overview surveys directing operational activities.

To detect and map smaller and more concentrated areas of bark beetle infestation, forest districts or licensees conduct more detailed aerial surveys. These surveys are normally completed at a scale of 1:20,000 using a helicopter with a Global Positioning System (GPS). A GPS position is taken at the centroid of an individual cluster of red attack trees. The information collected from helicopter GPS surveys is used primarily for expediting the deployment of field crews to find green attack in areas where suppression activities are recommended. An advantage over other survey methods is the low error of commission; the surveyor gets a good look at each crown and can differentiate between bark beetle and other damage agents such as flooding, mechanical damage or porcupine girdling. The disadvantage is that there may be errors of omission if the coverage of the helicopter-GPS survey is not systematic across areas of lodgepole pine forests. Furthermore, although it is very effective for small and localized area surveys at the early stage of infestation, it is prohibitively expensive when dealing with a beetle outbreak over a large area.

To map large areas of mountain pine beetle red attack, satellite remote sensing offers similar quality products to those listed above, complete with repeat coverage and consistent spatial scale at a variety of costs. Such data provides complementary characteristics to other approaches and could be used to scale small area estimates of timber supply and forest related land-use to larger areas where other data sources do not exist. The advantages of such a procedure are highlighted in the next section while a review and recommendations of all mountain pine beetle survey methods are presented in Wulder et al. (2005a).

1.3 The advantages of a data hierarchy

From a forest management perspective, estimates of the location and extent of mountain pine beetle red attack are critical, however the degree of precision required for these estimates varies according to the management objective (i.e., strategic, tactical, or operational) under consideration, and the nature of the infestation (i.e., endemic, incipient). The range of information requirements is matched by a hierarchy of different data sources that are currently used to map red attack damage (e.g., aerial overview surveys, helicopter surveys, aerial photography, and field surveys), with each data source offering a different level of detail on location and extent.

Maps of infestation location and extent drive mitigation and prediction activities related to attacks of mountain pine beetle. For example, the placement of field crews relies on accurate detection of insect

activities over large areas. Output from decision support models are improved through the inclusion of accurate maps of attack conditions. The integration of remotely sensed data with existing forest inventories in a Geographic Information System (GIS) environment generates value-added information for forest managers. In turn, the forest inventory provides a context for, and source of, validation data for the red attack information extracted from the remotely sensed data.

Remotely sensed data sources cannot replace existing methods of data collection; however, the image data may fit into the existing data hierarchy, providing complementary information or filling data gaps. Matching the appropriate data source to the information requirement reduces the complexity of data collection and processing, and ensures that the required level of detail is provided to address the management objectives specific to that level of the hierarchy. Furthermore, a data hierarchy is cost effective; relatively inexpensive low spatial resolution data sources may be used to guide the acquisition of more costly, higher spatial resolution data. For example, aerial overview sketch mapping (or relatively inexpensive, low spatial resolution satellite based remotely sensed data) can be used to provide a synoptic view of mountain pine beetle red attack damage at the landscape level and guide the acquisition of more costly, higher spatial resolution data.

1.4 Logistical issues to the mapping procedure

The proposed method to map mountain pine beetle has typically been used on individual Landsat frames (Skakun et al. 2003; Wulder et al. 2005b). The creation of a large-area product (provincial or national scale) involves the consideration of several logistical issues related to the mapping of a large area that are not often faced in small, research driven projects. Generating a consistent product over large areas involves the use of multiple scenes, collected on different dates and potentially in non-optimal seasons. In addition to data availability, the quality of available imagery can also be an issue. Imagery that is suitable for the detection and mapping of mountain pine beetle red attack damage must be free of cloud and haze, and must be acquired during the appropriate bio-window for mountain pine beetle.

Logistical issues that need to be considered and addressed when mapping a spatially and temporally extensive insect attack are listed below. The issues raised are addressed later in this report, as are the mapping procedure and the accommodations that can be made when deviations from the recommended protocol are required.

1. **Spatial Extent** Many scenes or portions of scenes may require processing depending on the size of the area. Determining the area to be mapped is therefore important. For instance, if full coverage of the attack is necessary, then methods which utilize change detection between scenes require two scenes of each area with two image dates. Cloud infill (described below) could also increase the number of scenes required to facilitate the complete spatial coverage.

2. **Timing** The damage caused by the beetle manifests over the period from July to September and persists through the winter to the following season. Imagery acquired prior to this optimal acquisition period will reflect an incomplete amount of cumulative damage caused by the insect for that year. However, biological considerations aside, physical conditions outside of this optimal window, such as sun angles, are not ideal for remote sensing of vegetation and as a result potential dates for image acquisition are significantly reduced. Shadows are also an issue, exacerbated by low sun angles beyond these dates, particularly in more northern locations.

3. **Costs** There are significant costs associated with a large-area mapping exercise. Both acquisition and processing costs associated with many scenes (or portions of scenes) are not trivial. In addition, there are costs associated with ancillary data processing (ground

truth), masks, and data management. Defining the mapping area is important to aid in the controlling of costs.

4. **Expertise** The procedure has been developed and described to enable the widest possible range of users to follow the process used. While there has been an attempt to keep the procedure simple, a level of GIS and remote sensing expertise will be required. Data processing of the ancillary data in the GIS environment is critical for the mask development and to facilitate the development of calibration and validation data sets. GIS skills are also required to ensure the required data management during and through to project completion. Remote sensing skills are required to ensure consistent processing of the imagery and perform the analysis (prior to the thresholding process). During the thresholding process user experience will reduce the time required for final threshold definition and validation iteration steps.

5. **Support data** The recommended process requires quality assured calibration and validation data. For red attack locations, heli-GPS or photo survey (known as a measle map) data is most appropriate as a source of calibration and validation data; aerial overview survey data is too coarse for calibration or validation purposes. The aerial overview survey data is more suitable to aiding the threshold development by providing an indication of the spatial extent of infestation. Obviously, ground data would be optimal for calibration and validation, yet it is acknowledged that these data are not systematically collected and supplied in a manner suitable for a project of this nature. Information on non-attack locations is also necessary. It is not possible to monitor for commission error (false-positives) without knowing where the trees are not attacked. This null-data is not collected by the surveys and since some of the surveys are non-systematic there is no guarantee areas without red attack have not been attacked (they may just not have been surveyed). Image processing techniques to define a non-attacked class for accuracy assessment purposes may inadvertently include some attacked trees or stressed trees. The heli-GPS data and the associated red attack tree counts per point provide an excellent and widely available source of calibration and validation data, especially when vet with the other available ancillary (e.g., forest inventory) or supplemental image information (e.g., using reflectance values to create masks).

6. **Optimal date for image acquisition** This is a critical issue for both biological (manifestation of attack) and physical issues (such as sun angles). The image acquisition impacts become both spatial (where scene edges meet) and temporal (the actual time gap between images, in years and seasonal representation).

7. **Multiple scenes** Multiple scenes create an additional cascading series of issues, for example, edge effects, image radiometric normalization, phenological differences, year differences, product definition, and data handling.

8. **Cloud cover** Cloud cover and related shadows obscure the ground cover, precluding affected pixels from analysis and subsequent mapping. Cloud and shadowed areas can be omitted from the final mapping, or some consideration of a maximum permitted allowable amount of cloud cover can be made. Currently clouded areas are excluded from the output resulting in gaps in the data that need to be treated as gaps or filled with some other available data source or additional imagery.

2.0 Enhanced Wetness Difference Index (EWDI) approach to mapping red attack

The infrared and short-wave infrared spectral channels of the Landsat sensor are known to be particularly sensitive to changes in forest structure. Image transformations that exploit changes over time in the infrared and short-wave infrared channels have shown success in mapping subtle forest changes related to insect disturbance (Price and Jakubauskas, 1998) through to stand replacing disturbances such as harvests (Cohen et al.1995; Wilson and Sader 2002) and fire burn severity (Epting et al. 2005). Single-date mapping of red attack is based upon the contrast between attacked stands and non-attacked stands. While reasonable classification accuracies may be found (73.3% ± 6.7%, $p = 0.05$), issues with omission and commission error may emerge (Franklin et al. 2003). To address limitations related to mapping a change feature with single date imagery, multi-date change detection approaches were developed and applied. Following examples in the literature highlighting the strength of approaches based upon the Tasselled Cap Transformation (TCT) for capturing change, the Enhanced Wetness Difference Index (EWDI) was developed (Skakun et al. 2003). The EWDI is the core of the recommended red attack mapping approach. This report describes the detailed protocol for implementing this procedure for red attack mapping and monitoring of mountain pine beetle infestation using a hierarchy of GIS and remote sensing data sources.

3.0 Methodology

The recommended mapping approach has a number of steps including pre-planning, image scene selection and image processing to produce a red attack map. The elements of the procedure to generate a red attack map are presented in Figure 1. Each of the steps are described in more detail in the following subsections.

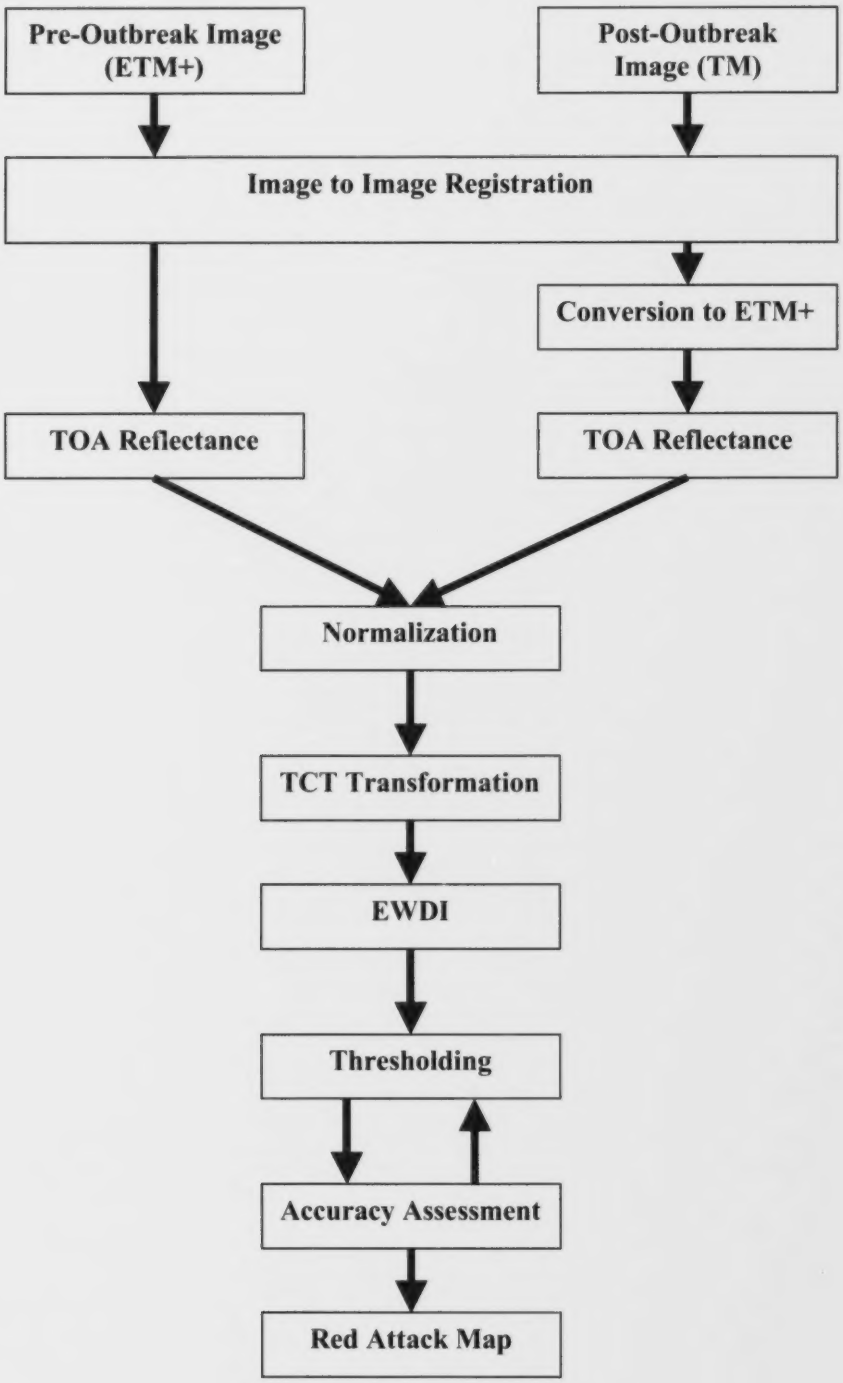

Figure 1. Summary of steps included in the processing flow to generate a map of mountain pine beetle red attack damage from two dates of Landsat TM/ETM+ imagery.

3.1 Required data

Given the data hierarchy that is required to accurately capture the location, spatial extent and magnitude of a mountain pine beetle outbreak, the methodology described in this report requires the following data sources (presented in Figure 2) to be available to the analyst.

Required Data Checklist for Red Attack Mapping of Mountain Pine Beetle:

Landsat Imagery

- 1 pre-infestation scene
- 1 post-infestation scene (preferably with 2 year lag)

Calibration Data

- Red attack damage (e.g., helicopter GPS or photo-based estimates of red attack [measle maps])
- Non-attack pine forest stands (e.g., ground based sources are preferred; however, image derived alternatives may be used in the absence of ground data)

Validation Data

- Red attack damage (e.g., helicopter GPS or photo-based estimates of red attack [measle maps])
- Non-attack pine forest stands (e.g., ground based sources are preferred; however, image derived alternatives may be used in the absence of ground data)

Forest Data

- Forest inventory information
- Forest harvesting information

Figure 2. Required data checklist for red attack mapping of mountain pine beetle.

The dates of imagery should be carefully selected. Generally, given the variability of fade rates, a two-year gap improves results as it allows all of the damage caused in one year to be captured (Wulder et al. 2005a). Calibration and validation for non-attack is more challenging, although image derived sources are available (e.g., use Normalized Difference Vegetation Index (NDVI) or TCT greenness). If photo surveys are available, those photos could be used to either vet and/or select samples of non-attack pine.

Forest inventory is used to identify the area covered by the host species. This is determined by selecting all the areas that have pine, in any layer. Harvesting information is used to identify harvesting which has occurred since the inventory was last updated. If necessary, additional harvesting information will be extracted from the imagery directly.

3.2 Scene selection

This section describes the procedure for optimal scene selection for red attack mapping. Optimal image characteristics include:

- Optimal months to capture change in tree crown colour from green to red: July, August, and September;
- Optimal temporal gap between annual images: two years.

Trees that are attacked by the beetle in one year will not typically fade from green to red until the growing season of the following year. The optimal time to capture this fade in foliage is during the summer months of July, August, and September of the year following attack. This is also the best time to collect remotely sensed imagery, since the sun angles are optimum during these months across most of Canada, and as a result, the amount of shadow in the imagery is reduced. Due to the variability in foliage fade rates, a two-year image gap is recommended in order to capture all of the damage associated with a single year's infestation (and enables use of imagery from the broader range of months). For example, if a stand was infested with the beetle in August, 2001, not all of the infested trees will have faded by the summer of 2002. An image collected in the summer of 2003 is preferred since the damage from the 2001 infestation will be more visible. Some trees, infested in 2002, will have faded by 2003 and also be captured in the image. These optimal image characteristics often require compromise when images are being selected. Non-optimal seasons or years will have an impact on the nature and quality of information captured.

The months and yearly gap recommended for use in the mapping procedure are based upon both biological and image acquisition considerations. It is acknowledged that imagery meeting these requirements will not always be available. Deviations from the suggested protocol will have impacts upon the accuracy of the final maps or on the amount of time it takes to implement the protocol. The between year gap, while recommended at 2 years, can be shortened to one year when the desired imagery is not available. Single year gaps will work best over areas where the attack levels on the landscape are high. Metadata should also track the images that are used to ensure that the nature of the product developed is known and understood by the subsequent users. The information need and the area being mapped can be considered to determine if a deviation from the mapping protocol is acceptable for a given area.

The recommended image selection series for a sample red attack map product are provided in Table 1. The product definition is a function of the gap between image dates, as this dictates how much attack was present on the landscape. In the ideal scenario, as discussed, the goal is to capture all the attack occurring for the year between the two dates of imagery. In the cases below, years may be substituted for the T = time notation. For example, if the desired mapping year to capture is 2003, T1 is 2002, T2 is 2004, with the recommended months of July, August, and September.

Table 1. Image selection criteria based on year and month combinations for mapping red attack.

Recommendation	Between year	Within year (month)
Ideal	T1; T2 = T1 + 2	July, August, September
Optional	T1; T2 = T1 + 1	June – October
Not recommended	A time gap greater than 3 or 4 years; this will vary by site.	Months earlier than June or later than October (with sun angles, attack stage, and snow cover being the key issues).

Applying this logic, the recommended sequence for mapping 2003 red attack conditions based on 2002 infestation would be as follows (beginning from the ideal, then altered to meet operational considerations):

1. 2002 – 2004; July – September
2. 2001 – 2004; July – September
3. 2003 – 2004; July – September
4. 2002 – 2003; July – September
5. 2002 – 2004; earlier than July or later than September

From this sequencing it is also clear that deviations in the year of detection are preferred over seasonal variations. The reduction in image radiometric quality for off-season imagery solely based upon sun angles and available solar radiation reduces the ability to capture changes clearly. Off-year imagery is typically preferred over off-season imagery for remote sensing mapping applications (Wulder et al. 2004b). The variance between attacked and non-attacked areas for these non-optimal seasons impacts the quality of mapping results and increases the processing time required. The biological considerations of fade rates further encourage maintenance of seasonal image selection recommendations to be as close as logistically possible.

Recent research has indicated that longer time intervals between images may be used to map locations of mountain pine beetle impacts, although there is decreasing accuracy as the time interval between images increases (Wulder et al. 2005c). As the time interval between images increases, additional change detection and disturbance attribution procedures may be required, as trees killed by mountain pine beetle will represent a range of attack stages (including both red and grey attack stages), with the spectral characteristics increasingly resembling non-attacked conditions. The condition of the individual trees and the site will also play a role in the success with which the damage can be detected over time. Site conditions, such as prolonged drought, can influence the rate at which the attacked trees will progress through the various attack stages (Safranyik, 2004) and this type of site-specific knowledge should be considered when detection and mapping is undertaken. The practical implications of these results suggest that in order to detect and map mountain pine beetle damage over a longer time period, multiple image pairs should be selected over the time period in question, rather than a single image pair representing the start and end years of the time period. For example, over the 1995 to 2001 period considered in Wulder et al. (2005c), a series of EWDIs generated from multiple image pairs may have been used (e.g., 1995-1997, 1997-1999, 1999-2001). Alternatively, if resources permit, annual image pairs (e.g., 1995-1996, 1996-1997, 1997-1998, etc.) may also be used or the pre-infestation image (1995) could be used as a baseline for multiple image pair analysis (e.g., 1995-1996, 1995-1997, 1995-1998 and so on).

3.3 Ancillary data preprocessing

There is a significant amount of GIS pre-processing that is required to generate masks that will restrict the image analysis and aid in vetting the calibration and validation data points. Some of the masks generated are described in detail below; all masks are summarized in Table 2.

The pine mask is designed to identify areas that have a pine component. The Vegetation Resource Inventory (VRI) data is used as a source for this information. The inventory is queried and any stands having pine in any of the top six species attributes are identified. All areas containing pine and potential host species are therefore identified. This helps to reduce variability in spectral values caused by non-forest and other species. The harvest masks are generated from provincial data and directly from the Landsat imagery.

Table 2. A summary of masks used for vetting calibration and validation data and for restricting image analysis and product output.

Mask	Description/purpose	Criteria	Code
pine	Identify forest inventory stands with a lodgepole pine component.	Select for 'PL' in species 1 through 6	pine = 1
harvest	British Columbia Ministry of Forests and Range provided a harvesting layer	Generated from Landsat time series	harvest = 1
harvest-add	Additional harvesting since British Columbia Ministry of Forests and Range data layer produced	Using band math, TOA5 – TOA4. Anything > 0.08 can be masked out	harvest-add = 1
cloud	Identify areas of cloud/haze for both image dates	Threshold TOA1 > 0.1*	cloud2004 = 1 cloud2002 = 1
dark	Identify dark objects (e.g., terrain shadow, cloud shadow)	Threshold TOA4 < 0.04*	dark2004 = 1 dark2002 = 1
bufpine	Buffer forest inventory polygons containing pine by 25 metres restricts points to interior of polygons; reduces variability of points found along the edge of stands	Buffer polygons (inside and out) by 25 metres; area inside buffers is coded as 25, area outside is NODATA	bufpine = 25
pl75	High-grade the lodgepole pine mask to identify only those pine stands with greater than 75% pine	Select where species_1 = 'PL' and species_1_pct > 75	PL75 = 'PL75'

*Values are provided as guidelines only, they will vary slightly by scene.

The pine masks and harvesting mask are used to vet the calibration and validation samples. Ground field observations which are located outside areas known to contain pine can mean the pine mask is incorrect, the ground-truth data contains positional inaccuracy, or that the stand which was identified as infested may have been harvested between the time the truth data was collected and when the image was acquired. Image pixels influenced by clouds and associated shadows should also be masked. Additional masks, designed to exclude undesirable pixels, are described in Table 2.

Generally, all of the masks listed in Table 2 have two primary functions: (i) to vet the calibration and validation data; and (ii) to restrict the spatial extent of the output product. The masking encourages and enables the processing of pixels to have change related to mountain pine beetle attack rather than a transition, for example, from forest to cloud shadow. The masks also aid in the selection of points for calibration, but excluded points impacted by clouds or salvage harvesting. False positives in the mapping of red attack are reduced through the mask application. The set of points remaining enables the interpretation of the results to be made under an assumption that the calibration and validation is not impacted by extraneous conditions. The use of an image-extent mask is common to reduce the image processing requirements by not processing no-data areas that are typically produced through the rotation or translation associated with geometric correction.

3.4 Image preprocessing

3.4.1 Assess quality/suitability of imagery

Free, archived, Landsat imagery are available from the Global Landcover Facility (University of Maryland), CEOCAT (the Canada Centre for Remote Sensing [CCRS] Landsat archive) or the World Wide Web at www.Landsat.org and often contain the best possible imagery for only one or two image dates. Other data providers hold much larger, higher quality collections with much better temporal cover-

age of Landsat data but the cost may be substantial for large area projects. Unfortunately, some of these archived images may contain some cloud or haze, which can have an impact on the detection of mountain pine beetle red attack damage. Small areas of haze and cloud can be masked out; however, where the area impacted by haze and cloud is large (more than 20% of the image), or where clouds and haze obscure important areas that require mapping, alternate imagery should be sought.

If the red attack product is being generated on a scene-by-scene basis, the edge matching of output will be a consideration after all of the required products are generated. To generate a product based on logical unit (e.g., forest district), some thought should be put into the best approach for production. For example, images may overlap, so a decision may be made to mosaic images together (after pre-processing, but before wetness calculation). Such mosaicking may help to reduce processing time and avoid duplication of analysis in overlapping image areas.

The imagery available in some Landsat archives is also orthorectified. When normalizing imagery, the radiometry must be known. When imagery is orthorectified (geometrically corrected to real-world coordinates and fit to elevation data) the digital numbers are altered in some manner, with the bulk of the differences found over areas with rugged terrain. To enable application of rigorous standardization and normalization prior to application of the standard TCT components, it must be ensured that the digital numbers (DN) for a given pixel in the ortho-imagery did not significantly deviate from the DN values found in raw imagery. The fact that the DNs of the ortho-imagery were only altered slightly and systematically from raw DNs enabled the application of standard calibration values to normalize the imagery, convert the Landsat-5 to Landsat-7 spectral radiometry, convert radiance values to top-of-atmosphere values, and subsequently apply the standard TCT transforms for Landsat-7 ETM+.

3.4.2 Geometric correction

Successful change detection requires accurate co-registration of the two image dates. An image-to-image correction must be undertaken between the two source images, using the older date as the master image and the newer date as the slave image. Common permanent features (e.g., road intersections, landmarks) found in both of the images should be used for the registration. A 2nd order polynomial transformation and nearest neighbour resampling are recommended, along with a target root mean square (RMS) error of less than half a pixel. A minimum of 15 ground control points (GCPs), well distributed throughout the spatial extent of the image, is recommended.

To improve productivity, sequential images collected on the same date and path may simply be mosaicked. For example, two images (Path/Row=49/22 and 49/23) can be stitched together, or ordered as one product from the data provider, increasing the data processing productivity by 50%. However, imagery acquired on different dates should not be mosaicked together without some consideration to scene normalization.

3.4.3 Conversion from TM to ETM+

Though the two Landsat sensors are compatible, they have different characteristics in configuration (e.g., band centre wavelength, band width), spectral response, and signal-to-noise ratio (Irish, 2000). To reduce the disparity between TM and ETM+ imagery, and to facilitate the application of the tasselled cap coefficients developed by Huang et al. (2002a), the TM images are first converted to ETM+ sensor radiometry. The conversion is achieved by applying a set of gains and offsets to the TM images. These gains and offsets, as listed in Table 3, were introduced by Vogelmann et al. (2001), and verified and applied by Huang et al. (2002b). Note that if two Landsat TM images are used to generate the EWDI, this conversion step is not required and TCT coefficients from Crist and Cicone (1984) should be used instead. Once the TM is converted to ETM+ equivalent, the remaining processing steps (e.g., conversion

to radiance, conversion to reflectance, normalization, and calculation of the tasselled cap transformation) are all completed on the ETM+ equivalent radiometric scale.

Table 3. Coefficients for conversion of Landsat TM to ETM+ equivalent.

Band	Gain	Offset
1	0.9398	4.2934
2	1.7731	4.7289
3	1.5348	3.9796
4	1.4239	7.0320
5	0.9828	7.0185
7	1.3017	7.6568

Equation 1 is used for this conversion:

$$Rad_i^7 = DN_i^5 \times Gain_i + Offset_i \quad (1)$$

where i: band number, for i = 1,2,3,4,5,7;

Rad_i^7: converted DN of band i;

DN_i^5: TM DN of band i to be converted;

$Gain_i$: gain of band i;

$Offset_i$: offset of band i.

3.4.4 Radiometric correction

Huang et al. (2002a) reported that pseudo-invariant objects can have different DN values between summer and fall/winter. Much of the differences are removed by converting the DN to at-satellite reflectance. Huang et al. (2002b) developed a conversion algorithm to covert the raw digital number (DN) to at-satellite reflectance for Landsat ETM+ data. Conversion of ETM+ DN numbers to top of atmosphere (TOA) reflectance is required to apply the tasselled cap coefficients developed by Huang et al. (2002a).

There are four steps involved in the process:

1. Mask out areas of the image containing valid data;
2. Convert «raw» DN values to at-sensor radiance;
3. Convert at-sensor radiance to TOA reflectance;
4. Scale TOA reflectance from #3 to 8-bit image channels.

Step 1: Mask out non-data areas of the image

To speed up processing, a mask of the valid image data is generated using band thresholding. This restricts calculation of TOA radiance and TOA reflectance to areas of real image data, and reduces the amount of processing time required to do the conversions. A simple way to generate this mask is to threshold all values in band 4 that are greater than 0.

Step 2: Convert "raw" DN values to at-sensor radiance

Twelve 32-bit channels should be created to hold the outputs of the following processing steps. The raw DN values are converted to radiance and output to a 32-bit channel, using equation 2 (Markham and Barker, 1986):

$$Rad_i = DN_i \times Gain_i + Offset_i \quad (2)$$

where i: band number, for i = 1,2,3,4,5,7;

Rad_i: TOA radiance of band i;

DN_i : DN of band i;

$Gain_i$: gain of band i;

$Offset_i$: offset of band i.

Note, depending on the Landsat product generation system (i.e., National Landsat Archive Production System - *NLAPS*, Landsat Ground Station Operations Working Group - LGSOWG) the user should consult the specific metadata files to determine the actual *Gain* and *Offset* used to scale the Landsat data to at-sensor radiance. If these coefficients are not available, the pre-launch calibration coefficients may be used resulting in an undetermined decrease in radiometric accuracy.

Step 3: Convert TOA radiance to TOA reflectance

The TOA radiance values from 2 are then converted to TOA reflectance, and output to a 32-bit channel, using equation 3 (Markham and Barker, 1986):

$$\text{Re } f_i = (Rad_i \times \pi \times d^2) \div (ESUN_i \times \cos(\theta)) \quad (3)$$

where i: band number, for i = 1,2,3,4,5,7;

Re f_i: TOA reflectance of band i;

Rad_i: TOA radiance of band i;

d : Earth-Sun distance in astronomical unit (Table 4);

$ESUN_i$: mean solar exoatmospheric irradiance of band i (Table 5);

θ : Sun elevation angle.

Table 4. Earth-Sun distance in astronomical unit (Source: Huang et al. 2002b).

Julian day[1]	Distance	Julian day	Distance	Julian day	Distance	Julian day	Distance	Julian day	Distance
1	.9832	74	.9945	152	1.0140	227	1.0128	305	.9925
15	.9836	91	.9993	166	1.0158	242	1.0092	319	.9892
32	.9853	106	1.0033	182	1.0167	258	1.0057	335	.9860
46	.9878	121	1.0076	196	1.0165	274	1.0011	349	.9843
60	.9909	135	1.0109	213	1.0149	288	.9972	365	.9833

[1]Julian day may be determined by accessing one of several Julian Day converters available on the World Wide Web (e.g. www.numerical-recipes.com/julian.html).

Table 5. ETM+ Mean solar exoatmospheric irradiances (Source: Huang et al. 2002b).

	Band 1	Band 2	Band 3	Band 4	Band 5	Band 7
ESUN watts/($m^2 \times \mu m$)	1969.00	1840.00	1551.00	1044.00	225.70	82.07

Sun elevation angle may be determined by using the sun elevation calculator (developed by NRCAN: www.hia-iha.nrc-cnrc.gc.ca/sunrise_adv_e.html). To use this calculator, you will need to know the latitude and longitude of the scene centre, as well as the time the image was acquired. If this information is not provided with the imagery, it may be obtained by locating the image in the CCRS Landsat archive (CEOCAT): ceocat.ccrs.nrcan.gc.ca. Follow the instructions for logging into this site using the default guest account and then browse the catalogue for your image(s).

Step 4: Scale TOA reflectance to 8-bit

TOA reflectance values will range from 0 to 1 in a 32-bit channel. To save disk space, and to facilitate the calculation of the tasselled cap transformation, the reflectance values are multiplied by 400 and then transferred to 8-bit channels (as per Huang et al. 2002a). This scaling will result in reflectance values greater than 0.6375 being truncated. Generally, this is not a concern for land cover applications, as the majority of land cover targets have reflectance values less than 0.6375 (Huang et al. 2002b). The coefficients developed by Huang et al. (2002a) must be applied to scaled TOA reflectance vales. Applying the ground reflectance factor based transformation directly to at-satellite reflectance images is not appropriate.

3.5 Image Normalization

This step is to remove the remaining discrepancies (snow, phenological differences, no data) between the two input images; the newer image date should always be normalized to the older image date.

Step 1: Generate a mask of snow and/or cloud cover

The objective of this step is to mask the unstable targets (e.g., cloud and snow) and no data areas in the image, in order to avoid selecting them as bright or dark pseudo-invariant targets for the image normalization (Figure 3). This mask may be generated using band thresholding. Band 4 is generally most suitable for selecting no data areas, while band 1 is useful for isolating areas of cloud and snow.

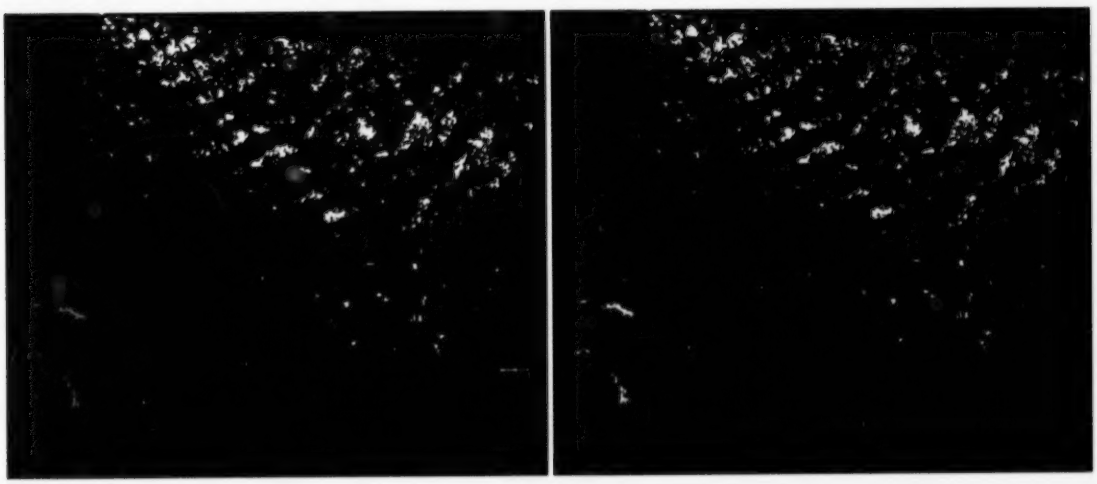

Figure 3. Illustration of the cloud/snow mask, with original imagery on the left side, with the generated cloud/snow mask shown on right in yellow.

Step 2: Combine the image masks generated for each image date

A separate mask of these unstable targets is generated for each image date, and then, both masks are combined (using simple bitmap arithmetic operations) to define the common area of possible suitable targets and unsuitable targets for both images.

Step 3: Normalize the newer image date to the older image date

The normalization was conducted using the relationship derived from the average dark and bright targets extracted from the input images (Hall et al. 1991):

$$Gain_i = (R_i^b - R_i^d) \div (S_i^b - S_i^d) \quad (4)$$

$$Offset_i = (R_i^d \times S_i^b - R_i^b \times S_i^d) \div (S_i^b - S_i^d) \quad (5)$$

$$\text{Re } f_i = Gain_i \times \text{Re } f_i + Offset_i \quad (6)$$

where i: band number, for i = 1,2,3,4,5,7;

$Gain_i$: gain of band i;

$Offset_i$: offset of band i;

R_i^b: average of the date 1 bright target TOA reflectance of band i;

R_i^d: average of the date 1 dark target TOA reflectance of band i;

S_i^b : average of the date 2 bright target TOA reflectance of band i;

S_i^d: average of the date 2 dark target TOA reflectance of band i;

Re f_i: TOA reflectance to be normalized of band i;

Re f_i: normalized TOA reflectance of band i

The targets selected for the normalization are those with the relative stable spectral signatures over the detection period. These targets are sometimes called pseudo invariant targets (PIT). Water is the ideal candidate of the dark target, while river bands, beaches, farmland or even clearcut areas can be selected as the bright targets. The number of target pixels used for the normalization is also important. Small number of pixels for each target may produce unstable normalization coefficients (gain and offset). The appropriateness of the target selection can be determined by examining the derived gain and offset.

3.6 Enhanced Wetness Difference Index

3.6.1 Tasselled Cap Transformation (TCT)

Tasselled Cap Transformation (TCT) compresses spectral data into a number of reduced bands associated with physical scene characteristics (Crist and Cicone 1984). Though this transformation was originally constructed for agricultural applications, it has been used to reveal some key forest attributes (Cohen et al, 1995). In this procedure, the wetness indices of the TCT are calculated based on the two-date Landsat images. The coefficients for the TCT transformation are different, depending on the input image. The coefficients employed here (Table 6) were derived by Huang et al. (2002a), which assume that the input image is calibrated to the ETM+ TOA reflectance. In addition, as the TOA values range from 0 to 1, they need to be rescaled to 8-bit by multiplying them by 400 before applying these coefficients (see Section 3.4.4).

Table 6. TCT transformation coefficients for ETM+ TOA data.

TCT index	Band 1	Band 2	Band 3	Band 4	Band 5	Band 7
Brightness	0.3561	0.3972	0.3904	0.6966	0.2286	0.1596
Greenness	-0.3344	-0.3544	-0.4556	0.6966	-0.0242	-0.2630
Wetness	0.2626	0.2141	0.0926	0.0656	-0.7629	-0.5388

$$WI = 0.2626 \times b_1 + .2141 \times b_2 + 0.0926 \times b_3 + 0.0656 \times b_4 - 0.7629 \times b_5 - 0.5388 \times b_7 \quad (7)$$

where *WI*: TCT wetness indices

b_i: TOA reflectance of band *i*, for *i* = 1,2,3,4,5,7

3.6.2 Wetness differencing

The EWDI is calculated with the following formula:

$$EWDI = W_1 - W_2 \quad (8)$$

where W_1 and W_2 are the TCT wetness indices of the date 1 and 2, respectively.

General speaking, large positive values indicate wetness loss, while the small EWDI values mean no change of wetness. The large negative EWDI values represent wetness gain. Therefore, the areas with large positive values in the EWDI image are likely to be the mountain pine beetle red attacked areas. However, mountain pine beetle red attack is not the only disturbance that results in a loss of wetness. Other forest management activities will all manifest as decreases in moisture.

3.6.3 Enhanced Wetness Difference Index (EWDI) visual display

The EWDI may be displayed visually by shooting the wetness index from the more recent date through the blue and green colour guns of the image display software. The wetness index for the older image date is then fired through the red gun, resulting in the display shown in Figure 4. Bright red areas in Figure 4 show a large moisture decrease and are representative of clearcuts (Point A). Mountain pine beetle infestation is characterized by a moderate moisture decrease and is shown in Figure 4 as a pink hue (Point B). Point C shows an old clearcut area revealing a moderate moisture increase due to regenerating vegetation.

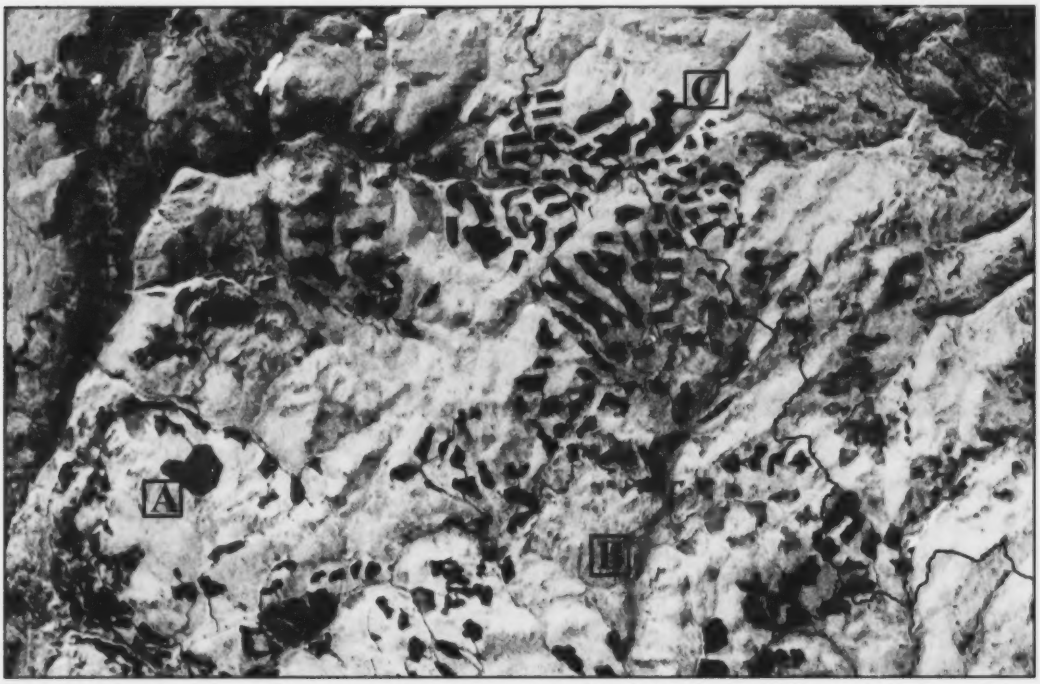

Figure 4. A sample of the EWDI from southern British Columbia. Red indicates a decrease in moisture from 2002 to 2004, blue indicates an increase in moisture and white indicates no change. Point A shows a large moisture decrease in a clearcut area, B shows an area of mountain pine beetle infestation, and C shows a moisture increase due to regenerating vegetation in an old clearcut.

3.6.4 Threshold determination

The EWDI values of the attacked and non-attack pixels can be approximated by the Gaussian distribution, and can be separated by using thresholding (Skakun et al. 2003). As shown in Figure 4 there are a range of EWDI values that can be linked to clearcuts, forest regeneration and mountain pine beetle infestation. To determine the EWDI thresholds, calibration and validation data are required for both red attack and non-attack pine stands. The red attacked validation data should be identified from helicopter GPS or other survey data sources. It is suggested to allot 50% of this data to calibration and 50% to validation. The non-attack truth can be derived from the pine-dominated (PL75 mask) pixels with the largest NDVI values calculated based on the date-2 (most recent) image. In Figure 5, distributions for red attack (dashed line) and "non-attack" (solid line) samples are presented. In the EWDI display, changes from harvests are found as moisture increases above red attack, with other subtle changes and non-change features found below red attack.

The development of the EWDI thresholds is an iterative process. In order to be consistent with the process outlined by Skakun et al. (2003), the optimal threshold values determined by Skakun et al. (2003) should be used as a starting point. The threshold can then be varied, up and down, using the calibration sets for non-attack and red attack sites. The distribution of points for each of the non-attack and red attack calibration points can be observed to provide insights on where to place the thresholds. Once the threshold has been set, the accuracy of the output can be verified using the reserved validation data.

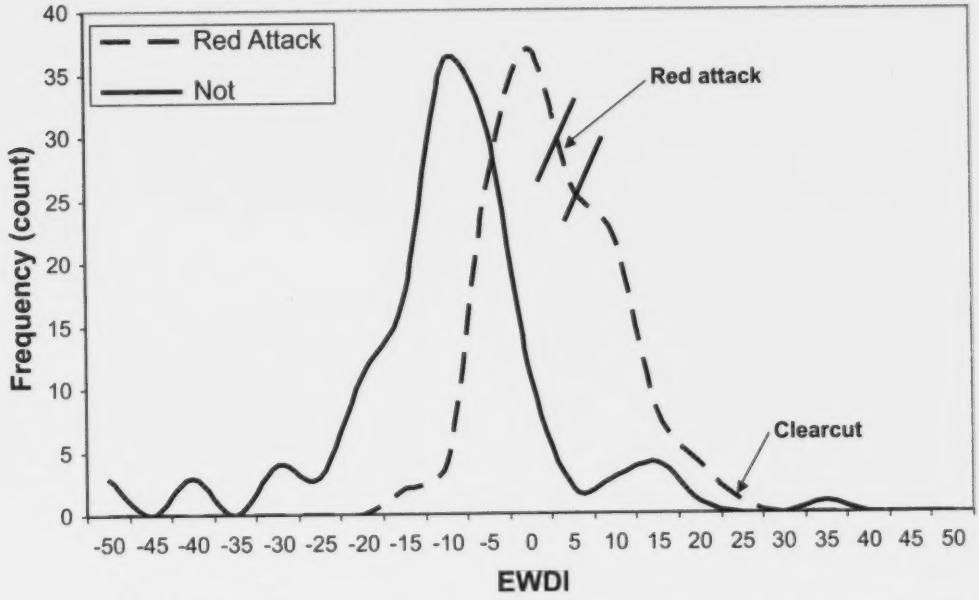

Figure 5. Generalized distributions capturing the EWDI values representative of red attack pixels (dashed line) and non-attack pixels (solid line). The thresholding notion is also illustrated, with a range of EWDI values categorized as red attack.

3.7 Accuracy assessment

The map products created as a result of using mountain pine beetle survey data with Landsat data can be subjected to an accuracy assessment. A transparent and robustly applied accuracy assessment provides a level of confidence to users of the map products. Specifically, an accuracy assessment provides information on the success of the detection methods used and identifies possible sources of error. It is also valuable for comparing and evaluating different mapping techniques and in the development of new methods. An error matrix is a useful mechanism for summarizing results and facilitating the calculation of accuracy measures; an example generated for a hypothetical mountain pine beetle is presented in Table 7. An error matrix enables a quantitative comparison of classes, or attributes, between independent validation data with the mapped results (Congalton and Greene 1999). The comparison may be between the results of an analysis based upon remotely sensed data and field data, or between outcomes using different methodologies. This type of accuracy assessment can also be applied to the results of non-digital methodologies including aerial surveys and photo-interpretation.

Table 7. Example of error (confusion) matrix for a hypothetical mountain pine beetle detection study with two classes.

	Ground-validated non-attack trees	Ground-validated attacked trees	Sum	User's accuracy[1]
Remotely sensed non-attack trees	96	4	100	96%
Remotely sensed attacked trees	3	97	100	97%
Sum	99	101	200	Overall accuracy
Producer's accuracy[1]	96.9%	96%		96.5%

[1]See text for definition.

In Table 7, the overall accuracy is the percent of correctly classified sample points along the diagonal of the matrix divided by the total (e.g., 193/200 = 96.5%). The overall accuracy provides a general indication of the accuracy of the map if all classes were of equal importance. If all classes were not of equal importance, the overall accuracy may misrepresent the accuracy of the map. In our example, there were an equal number of ground-validation sites that were non-attack versus attack trees, thus, the overall accuracy was not dominated by the accuracy of one class alone. When the sample sizes are the same the overall accuracy represents a valid indication of accuracy for the map as a whole.

Each individual class had two measures of accuracy: producer's and user's. The producer's accuracy is the percent of reference sites for a particular class that were correctly classified during the thresholding procedure. For example, in Table 7, 96% of the attacked trees in the study area (as identified by the reference source) were identified by the remote sensing method (e.g., 97/101=96%). The corollary of the producer's accuracy was the omission error: the number of reference sites, for a particular class which were omitted from the remotely sensed class (e.g., 4/101=4%). Continuing our example, 4% of the attacked trees were missed by the remote sensing method. The user's accuracy is the percent of remotely sensed sites that were correctly classified and from our example, 97% of attacked trees were correctly mapped (e.g., 97/100=97%). The corollary of the user's accuracy was the commission error: the number of reference sites for a particular class that were erroneously included in the remotely sensed class. For our example, 3% of attacked trees were mistakenly identified as non-attack trees (e.g., 3/100=3%). The most useful single indicator of accuracy for an attack map is the user's accuracy for the attack class; also known as the true-positive rate (Kohavi and Provost 1998).

Measures of accuracy clearly depend on the quality and quantity of the validation data available. For example, the sites used to test the accuracy should not have been previously used in the classification process for calibration, or the accuracy assessment may be erroneously high (Congalton and Greene 1999). The size of the sampling unit should reflect the resolution of the final product (Stehman and Czaplewski 1998). If the sampling unit is much smaller than, for example, the pixel size, it is unclear if matching classes is due to the site being within the pixel or other pixel content. Furthermore, the sampling design should reflect the importance of different classes. If all classes are equally important then a stratified sample design could be applied, with the number of samples proportional to the area of each class. If one class is more important, then at least an equal number of samples should be taken in that class, even if it is rare on the landscape.

There are a range of factors that must be considered to develop a statistically robust accuracy assessment (Cochran 1977). The interpretation of the subsequent accuracy of an attack map is linked to the study design. For instance, the classification scheme used in the mapping must be the same as the one used for the testing or validation data (Congalton and Greene 1999). The sample unit and the number of samples collected are a function of the classification scheme, the minimum mapping area, the extent of the mapping area, and the desired width of the confidence intervals (Congalton and Greene 1999). The sample design should, first and foremost, select samples without bias so the accuracy assessment is valid over the entire map area. Spatial autocorrelation can create a bias in the estimate of accuracy if it is not taken into account as part of the sampling design (Congalton and Greene 1999). Simple random sampling and stratified random sampling are the most robust sampling designs from a statistical perspective (Congalton and Green 1999). A valid accuracy assessment is most likely to occur if the design is based on an understanding of the characteristics of the remotely sensed data, the classification scheme, the processing methodology, and the biology related to the apparent forest condition.

In order to assess the effectiveness of the red attack mapping procedure, the method was applied to three test sites and an accuracy assessment was performed. The three test sites were located in south and central British Columbia, Canada, and are presented in Figure 6.

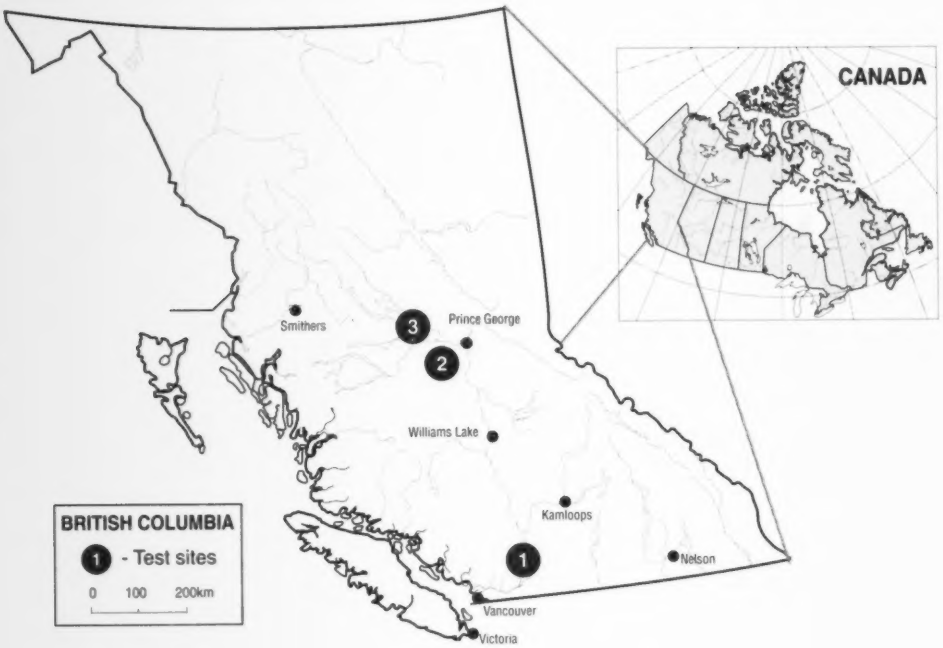

Figure 6. Location of test sites in British Columbia, Canada.

Table 8. Classification accuracies of the EWDI procedure for three test sites.

Test site	Characteristics	Red attack accuracy	Error bound
Test site #1	Low levels of attack	60%	48% - 73%
Test site #2	Non-optimal imagery	62%	56% - 76%
Test site #3	Optimal conditions	78%	70% - 92%

Site #1 was selected as an area representative of a light infestation located in a relatively pure lodgepole pine forest. Site #2 was selected as an example of a more severe infestation case within a heterogeneous forest species composition. Due to the lack of high quality imagery available for this area, a non-optimal image date had to be selected as the pre-disturbance image (October 22, 2002). Site #3 was characteristic of a moderate infestation site located in a relatively pure lodgepole pine forest.

Accuracies for the EWDI procedure applied to several case studies with different characteristics are presented in Table 8.

Test Site #1 was characteristic of low levels of red attack damage and suitable multi-temporal imagery was available for EWDI analysis. The reported true positive accuracy for red attack damage at this site was 60%. Test Site #2 was characterized by heavy red attack damage and non-optimal imagery was used in the EWDI procedure. In this case, two images (October 22, 2002 and August 16, 2004) were used to capture red attack damage in 2003, with the October image containing significant amounts of snow cover. The true positive accuracy of red attack damage detection using this sub-optimal imagery was 62%. Lastly, the true positive accuracy obtained at Test Site #3, which had moderate red attack damage and optimal imagery for the EWDI procedure, was approximately 78%.

In a red attack mapping project, a target for accuracy can be specified with desired confidence intervals. For example, a target of 70% ± 10% may be considered an appropriate range for a red attack map

produced by the EWDI procedure. The establishment of such a target can serve many useful functions in the context of a large area mapping project:

1. The accuracy target can be used to guide the iteration of the EWDI threshold values;
2. In product development mode, the target can be used as a performance measure or benchmark, against which the consistency of the red attack outputs produced for different areas can be compared and assessed;
3. The accuracy target, in combination with confidence intervals, can facilitate the use of the detection and mapping protocol under non-optimal conditions; hence, rather than modifying the protocol to suit the conditions, the impact of the non-optimal conditions can be accounted for relative to the target accuracy and confidence intervals.

3.8 Level of effort

In order to break down the level of effort associated with each task of this mapping protocol, the suggested level of effort values are presented by main protocol stage in Table 9. These suggested values, based upon experience in using Landsat data to map mountain pine beetle attack, can provide insights when planning costs or to ensure that adequate time is apportioned for undertaking the mapping.

Table 9. Estimated amount of effort associated with each of the tasks required to implement the protocol outlined in this report.

Task	Description	Level of effort
Acquisition	Compilation of all required data sources including imagery, forest inventory, mountain pine beetle survey data (e.g. aerial overview survey, heli-GPS).	15%
Ancillary data processing	Mask generation and calibration / validation data creation: • generation of masks from forest inventory and imagery (as appropriate) (e.g., cloud, shadow, pine, harvest) • compilation, selection, and vetting of calibration and validation data sources	10%
Image processing	Image geo-radiometric processing: • geometric correction (ensuring an image-to-image match, even for ortho-correct imagery) • radiometric correction (conversion to radiance, conversion to reflectance, normalization, conversion from TM to ETM+ as necessary). • computation of the TCT for each image • differencing of wetness imagery derived from the TCT	30%
Threshold determination	Iterative process using the calibration points for both red attack and non-attack. Optimal threshold values for red attack will maximize true positive and minimize commission errors.	30%
Validation	Reserved validation points are used to assess the final output. Accuracy is reported using an error matrix.	15%

4.0 Recommendations

Some of the following recommendations have been described in previous sections of this report; however, the key issues and recommendations for the proposed mapping protocol are summarized here for the benefit of the reader.

Project pre-implementation planning:

- Correct and accurate selection of the study area is critical to ensure image acquisition costs are minimized.
- The recommended approach provides better results over areas with more homogeneous and extensive attack.
- Careful consideration of those areas of the infestation where a spatially explicit mapping of red attack damage will provide the greatest benefit to the end-user (e.g., areas with significant amounts of pine volume impacted by the beetle).
- The Landsat Worldwide Reference System (WRS) image database and aerial overview survey data provide for an excellent planning tool, relating both spatial and temporal attribute conditions for the image locations.

Scene selection issues:

- Avoid scenes with excessive cloud and haze.
- Mask out cloud, cloud shadows, haze, topographic shadows, and snow cover.
- Where possible, ensure all acquired image is obtained for optimal dates to avoid additional problems. It can be expected that alterations to the scene selection criteria will possibly result in both an increase in time required for analysis (due to additional processing or analysis) and a reduction in accuracy of the final product.
- Attempt to adhere to the recommended optimal months of July, August, and September.
- Images taken late in the year can have a lower dynamic range (particularly true in northern areas). This reduction in spectral variance reduces detectability and will likely result in more difficulty in defining the threshold, due to increases spectral overlap between red attack and non-attack classes.
- Attempt to adhere to the two-year image gap as recommended where possible. Not using the two-year gap is less of an issue over areas where the attack levels are high.

Geometric registration:

- Geometric matching of the two scenes is a critical pre-processing step, even with the orthorectified imagery, to ensure that that the images are properly co-registered.
- After the scene-to-scene co-registration, quality assurance should be followed. The quality assurance can be undertaken by looking at bands of different dates through different guns to capture and exaggerate offset effects.
- The root mean square error (RMS) acceptable should be less than half a pixel (RMSE of < 0.5).

Radiometric calibration:

- Undertaking the radiometric correction makes the interpretation of the EWDI easier and increases the possibility of using standard values at the thresholding stage across the entire study area.
- There is a need to perform a quality assurance step following the radiometric corrections.
- Depending upon the image dates and locations, it can be time consuming to find acceptable pseudo-invariant targets.

Calibration/Validation:

- Calibration and validation are critical components of any remote sensing study.
- Aerial overview survey data can aid in guiding analysts to an expected amount of red attack for a given year over a particular area.
- Heli-GPS or measle mapping data can be vet with image based and ancillary data masks to improve the quality of the points used by confirming the characteristics of the points (e.g., not harvested, not on a road, etc.).

Masks:

- Critical for vetting calibration and validation points and for use in some of the radiometric pre-processing steps.
- Masks are used to exclude pixels that are not appropriate for inclusion in the analysis, such as those obscured by cloud, haze, or shadows.
- Masks are also used, as described above, to improve and ensure the quality of the calibration and validation data used.

Edge-matching issues:

- Image normalization reduces edge-matching issues.
- Time should be left for checking and subsequent addressing of any edge-effects that are evident.
- Generalized products, such as the 1 ha grid or polygon representations of internal attack conditions, are recommended.

EWDI Thresholding:

- Start with established ranges, alter with information garnered from distribution of EWDI values in the calibration data.
- Iterate with different possible threshold values to determine the best possible values.
- An efficient template can be established in a spreadsheet to facilitate the examination of various threshold scenarios.
- Need to balance threshold performance (e.g., accuracy measures) against total area mapped. Aerial overview survey data can serve as a useful indicator, although expect these numbers to be somewhat different (Wulder et al. 2005b). One hundred percent of the area could be mapped as red attack to get a 100% true positive rate for red attack (indicating again the importance of a "non-attack" pixel validation dataset to inform on commission error).
- Analysts need to maintain flexibility in values used in the thresholding. Previously used values can be used as a guide, but the imagery, geography, species mixtures, site conditions, etc., can all slightly impact the values. The radiometric correction of the images is an attempt to make the required changes to the threshold values as slight as possible. Analysts can use previously defined thresholds as a guide for the mapping of subsequent imagery.

5.0 Conclusions

An approach for mapping red attack stage of mountain pine beetle attack has been presented in this report. The core approach includes the following steps to address logistical and processing issues specific to this large area mapping project using remotely sensed data:

- image geometry, radiometric normalization
- EWDI threshold determination and iteration
- ancillary data requirements
  - o mask development
  - o calibration and validation data
- accuracy assessment.

It is clear from the remote sensing based EWDI red attack mapping approach that image availability and image quality are going to be significant issues in the implementation of this method (or any method).

The research on the use of satellite imagery to map the red attack stage of mountain pine beetle attack completed over last 5 years presented a useful basis for recommending a red attack mapping approach for large areas. The core method, generated from this research, is robust and produces useful map products. Map products may subsequently be processed to generate custom information layers in either raster or vector forms. The procedure presented is designed to be appropriate for application by range of user experience levels. The level of detail provided in this report is intended to provide clear direction for those interested in replicating the approaches presented.

Throughout the report, there has been a conscious effort to be clear about what the issues impacting a project of this nature. Transparency has been applied in the recommended approaches to follow when deviations from the standard procedure are necessary. The issues that are of major concern are the spatial and temporal nature of red attack on the landscape, physical limitations due to sun-angles and topography, as well as image and remote sensing issues. While these issues exist, and are worth noting, suggestions in this report illustrate that even when non-optimal conditions exist, useful maps of red attack can still be developed.

Consideration of the needs for the satellite based red attack data should be revisited prior to planning any large area implementation. If a key goal of the satellite based mapping is to capture the spatial heterogeneity of attack, could samples of satellite imagery be used to calibrate the level of attack in particular regions, which could then be applied over those areas that have not been mapped, but which have similar forests and attack levels? The current procedure can provide change in attack levels over time through repeated mapping. The option to operate on samples of imagery rather than performing a complete census of the infestation area may enable greater temporal coverage, at the cost of spatial coverage. The driver for the spatial coverage over temporal coverage should be clear.

When looking forward to potential new imagery, rather than being constrained to archival imagery, high spatial resolution satellite mapping provides a unique data alternative. Stand-level red attack mapping for low and moderate levels of attack has been demonstrated (White et al. 2005) and may be an alternative for future attack, especially when forming a component of a multi-stage, sample based, monitoring program.

6.0 Acknowledgements

This protocol was developed as a joint project between The Government of British Columbia, Ministry of Forests and Range (BCMoFR) and the Government of Canada's Mountain Pine Beetle Initiative. The Mountain Pine Beetle Initiative is a six-year, $40 million program administered by Natural Resources Canada, Canadian Forest Service. Additional information on the Mountain Pine Beetle Initiative may be found at: mpb.cfs.nrcan.gc.ca/. Ann Morrison, of the Update Section of the Forest Analysis and Inventory Branch of BCMoFR, is thanked for insights that supported and improved the analysis undertaken in this report. Rick Baker, Manager of the Update Section, is thanked for recognizing the need to develop a transparent mountain pine beetle mapping protocol and for supporting the project's implementation.

7.0 References

Amman, G.D. 1982. The mountain pine beetle – identification, biology, causes of outbreaks, and entomological research needs. Pages 7-12 *in* D.M. Shrimpton, editor. Proceedings of the joint Canada/USA workshop on mountain pine beetle related problems in western North America, Environment Canada, Canadian Forestry Service, Pacific Forest Research Centre, Victoria, B.C. Information Report BC-X-230. 87 p.

Amman, G.D.; Cole, W.E. 1983. Mountain pine beetle dynamics in lodgepole pine forests part 2: Population dynamics. USDA Forest Service, Ogden UT, GTR-INT-145, 59 p.

Ballard, R.G.; Walsh, M.A.; Cole, W.E. 1982. Blue-stain fungi in xylem of lodgepole pine: a light microscope study on extent of hyphal distribution. Canadian Journal of Botany 60:2334-2341.

Ballard, R.G.; Walsh, M.A.; Cole, W.E. 1984. The penetration and growth of blue-stain fungi in the sapwood of lodgepole pine attacked by mountain pine beetle. Canadian Journal of Botany 62:1724-1729.

Berryman, A.A.; Raffa, K.F.; Millstein, J.A.; Stenseth, N.C. 1989. Interaction dynamics of bark beetle aggregation and conifer defence rates. Oikos 56:256-263.

British Columbia Ministry of Forests and Range. 2006. Online: www.for.gov.bc.ca/hfp/mountain_pine_beetle/facts.htm. Accessed January, 2006.

British Columbia Ministry of Forests. 1995. Bark beetle management guidebook. Forest Practices Code, Forest Practices Branch, Victoria, BC. 45 p.

Carroll, A.L.; Safranyik, L. 2004. The bionomics of the mountain pine beetle in lodgepole pine forests: establishing a context. Pages 21-32 *in* Shore, T.L., Brooks, J.E., Stone, J.E., eds. Mountain Pine Beetle Symposium: Challenges and Solutions, October 30-31, 2003, Kelowna, British Columbia, Canada. Natural Resources Canada, Canadian Forest Service, Pacific Forestry Centre, Victoria, B.C. Information Report BC-X-399. 298 p.

Carroll, A.L.; Taylor, S.W.; Régnière, J.; Safranyik, L. 2004. Effects of climate change on range expansion by the mountain pine beetle in British Columbia. Pages 223-232 *in* Shore, T.L. Brooks, J.E., Stone, J.E., eds. Mountain Pine Beetle Symposium: Challenges and Solutions, October 30-31, 2003, Kelowna, British Columbia, Canada. Natural Resources Canada, Canadian Forest Service, Pacific Forestry Centre, Victoria, B.C. Information Report BC-X-399. 298 p.

Cochran, W.G. 1977. Sampling techniques. 3rd edition. Wiley and Sons, New York, NY. 428 p.

Congalton, R.; Green, K. 1999. Assessing the accuracy of remotely sensed data: Principles and practices, New York: CRC Press. 131 p.

Cohen, W.B.; Spies, T.A.; Fiorella, M. 1995. Estimating the age and structure of forests in a multi-ownership landscape of western Oregon, U.S.A. International Journal of Remote Sensing 16:721-746.

Crist, E. P.; Cicone, R. C. 1984. A physically-based transformation of Thematic Mapper data – the TM Tasselled Cap. IEEE Transactions On Geoscience and Remote Sensing GE-22, 256-263.

Epting, J.; Verbyla, D.; Sorbel, B. 2005. Evaluation of remotely sensed indices for assessing burn severity in interior Alaska using Landsat TM and ETM+. Remote Sensing of Environment 96:328-339.

Franklin, S.; Wulder, M.; Skakun, R.; Carroll, A.L. 2003. Mountain pine beetle red attack damage classification using stratified Landsat TM data in British Columbia, Canada. Photogrammetric Engineering and Remote Sensing 69:283-288.

Furniss, M.M.; Schenk, J.A. 1969. Sustained natural infestations by the mountain pine beetle in seven new *Pinus* and *Picea* hosts. Journal of Economic Entomology 62:518-519.

Hall, F.G.; Strebel, D.E.; Nickeson, J.E., Goetz, S.J. 1991. Radiometric rectification: Toward a common radiometric response among multi-date, multi-sensor images. Remote Sensing of Environment 35:11-27.

Henigman, J.; Ebata, T.; Allen, E.; Holt, J.; Pollard, A.,eds. 1999. Field guide to forest damage in British Columbia. British Columbia British Columbia Ministry of Forests, Victoria, B.C., Canada.

Hill, J.B.; Popp, H.W.; Grove, A.R. Jr. 1967. Botany: A textbook for colleges, 4th edition. McGraw-Hill Book Co., Toronto, ON.

Huang, C.; Wylie, B.; Homer, C.; Yang, L.; Zylstra, G. 2002a. Derivation of a tasseled cap transformation based on Landsat-7 at-sensor reflectance. International Journal of Remote Sensing 23:1741 – 1748.

Huang, C.; Zhang, Z.; Yang, L.; Wylie, B.; Homer, C. 2002b. MRLC 2001 Image Preprocessing Procedure, USGS White Paper. Available online: landcover.usgs.gov/pdf/image_preprocessing.pdf. Accessed January, 2006.

Irish, R. R. 2000, Landsat-7 science data user's handbook: ltpwww.gsfc.nasa.gov/IAF/handbook/handbook_toc.html, National Aeronautics and Space Administration. Accessed January, 2006.

Kohavi R.; Provost, F. 1998. Glossary of terms. Machine Learning 30:271-274.

Markham, B. L.; Barker, J. L. 1986, Landsat MSS and TM post-calibration dynamic ranges, exoatmospheric reflectances and at-satellite temperatures. EOSAT Landsat Technical Notes 1:3-8.

Mathre, D.E. 1964. Pathogenicity of *Ceratocysis ips* and *Ceratocystis minor* to *Pinus ponderosa*. Contributions of the Boyce Thompson Institute 22:363-388.

Price, K. P.; Jakubauskas, M. E. 1998. Spectral retrogression and insect damage in lodgepole pine successional forests. International Journal of Remote Sensing 19:1627-1632.

Reid, R.W. 1961. Moisture changes in lodgepole pine before and after attack by the mountain pine beetle. Forestry Chronicle 37:368-375.

Safranyik, L.; Shrimpton, D.M.; Whitney, H.S. 1974. Management of lodgepole pine to reduce losses from the mountain pine beetle. Government of Canada. Department of the Environment. Canadian Forest Service, Pacific Forest Research Centre, Victoria, B.C. Forestry Technical Report 1.

Safranyik, L.; Shrimpton, DM.; Whitney, H.S. 1975. An interpretation of the interaction between lodgepole pine, the mountain pine beetle, and its associated blue stain fungi in western Canada. Pages 406-428 *in* Baumgartner, D.M., ed. Management of lodgepole pine ecosystems. Washington State University Cooperative Extension Service, Pullman, WA.

Safranyik, L. 2004. Mountain pine beetle epidemiology in lodgepole pine. Pages 33-40 *in* Shore, T.L. Brooks, J.E., Stone, J.E., eds. Mountain Pine Beetle Symposium: Challenges and Solutions, October 30-31, 2003, Kelowna, British Columbia, Canada. Natural Resources Canada, Canadian Forest Service, Pacific Forestry Centre, Victoria, B.C., Information Report BC-X-399. 298 p.

Skakun, R. S.; Wulder, A. M.; Franklin S.E. 2003. Sensitivity of the thematic mapper enhanced wetness difference index to detect mountain pine beetle red attack damage. Remote Sensing Environment 86:433-443.

Smith, R.H.; Cramer, J.P.; Carpender, E. 1981. New record of introduced hosts for the mountain pine beetle in California. USDA Forest Service, Pacific Southwest Forest and Range Experiment Station, Berkeley, CA, Research Note PSW–354. 3 p.

Solheim, H. 1995. Early stages of blue stain fungus invasion of lodgepole pine sapwood following mountain pine beetle attack. Canadian Journal of Botany 73:70-74.

Stehman, S.; Czaplewski, R. 1998. Design and analysis for thematic map accuracy assessment: Fundamental principles. Remote Sensing of Environment 64:331-344.

Taylor, S.W.; Carroll, A.L. 2004. Disturbance, forest age, and mountain pine beetle outbreak dynamics in BC: A historical perspective. Pages 41-51 *in* T.L. Shore, J.E. Brooks, and J.E. Stone, eds. Mountain Pine Beetle Symposium: Challenges and Solutions, October 30-31, 2003, Kelowna, British Columbia, Canada. Natural Resources Canada, Canadian Forest Service, Pacific Forestry Centre, Victoria, B.C., Information Report BC-X-399. 298 p.

Vogelmann, J. E.; Helder, D.; Morfitt, R.; Choate, M.J.; Merchant, J.M.; Bulley, H. 2001. Effects of Landsat-5 Thematic Mapper and Landsat-7 Enhanced Thematic Mapper Plus radiometric and geometric calibrations and corrections on landscape characterization. Remote Sensing of Environment 78:55-70.

White, J.; Wulder, M.A.; Brooks, D.; Reich, R.; Wheate, R. 2005. Detection of red attack stage mountain pine beetle infestation with high spatial resolution satellite imagery. Remote Sensing of Environment 96:340-351.

Wilson, E.H.; Sader, S.A. 2002. Detection of forest harvest type using multiple dates of Landsat TM imagery. Remote Sensing of Environment 80:385-396.

Wulder, M. A.; Dymond, C. C.; Erickson, B. 2004a. Detection and monitoring of the mountain pine beetle. Natural Resources Canada, Canadian Forest Service, Pacific Forestry Centre, Victoria, B.C. Information Report BC-X-398. 28 p.

Wulder, M. A.; Franklin, S.; White, J. 2004b. Sensitivity of hyperclustering and labeling land cover classes to Landsat image acquisition date. International Journal of Remote Sensing 25:5337-5344.

Wulder, M. A.; Dymond, C. C.; White, J.C. 2005a. Remote sensing in the survey of mountain pine beetle impacts: Review and recommendations. Natural Resources Canada, Canadian Forest Service, Pacific Forestry Centre, Victoria, B.C. Information Report BC-X-401. 55 p.

Wulder, M.A.; Skakun, R.S.; Franklin, S.E.; White, J.C. 2005b. Enhancing forest inventories with mountain pine beetle infestation information. Forestry Chronicle 81:149-159.

Wulder, M.A.; Skakun, R.S.; Dymond, C. C.; Kurz, W.A.; White, J.C. 2005c. Characterization of the diminishing accuracy in detecting forest insect damage over time. Canadian Journal of Remote Sensing 31:1-11.

Yamaoka, Y.; Swanson, R.H.; Hiratsuka, Y. 1990. Inoculation of lodgepole pine with four blue-stain fungi associated with mountain pine beetle, monitored by a heat pulse velocity (HPV) instrument. Canadian Journal of Forest Research 20:31-36.

Canadian Forest Service Contacts

For more information about the Canadian Forest Service, visit our website at
www.nrcan.gc.ca/cfs-scf/
or contact any of the following Canadian Forest Service establishments

(1) Atlantic Forestry Centre
P.O. Box 4000
Fredericton, NB E3B 5P7
Tel.: (506) 452-3500 Fax: (506) 452-3525
atl.cfs.nrcan.gc.ca/

Atlantic Forestry Centre – District Office
Sir Wilfred Grenfell College Forestry Centre
University Drive
Corner Brook, Newfoundland A2H 6P9
Tel.: (709) 637-4900 Fax: (709) 637-4910

(2) Laurentian Forestry Centre
1055 rue du P.E.P.S., P.O. Box 3800
Sainte-Foy, PQ G1V 4C7
Tel.: (418) 648-5788 Fax: (418) 648-5849
www.cfl.scf.rncan.gc.ca/

(3) Great Lakes Forestry Centre
P.O. Box 490 1219 Queen St. East
Sault Ste. Marie, ON P6A 5M7
Tel.: (705) 949-9461 Fax: (705) 759-5700
www.glfc.cfs.nrcan.gc.ca/

(4) Northern Forestry Centre
5320-122nd Street
Edmonton, AB T6H 3S5
Tel.: (403) 435-7210 Fax: (403) 435-7359
nofc.cfs.nrcan.gc.ca/

(5) Pacific Forestry Centre
506 West Burnside Road
Victoria, BC V8Z 1M5
Tel.: (250) 363-0600 Fax: (250) 363-0775
www.pfc.cfs.nrcan.gc.ca/

(6) Headquarters
580 Booth St., 8th Fl.
Ottawa, ON K1A 0E4
Tel.: (613) 947-7341 Fax: (613) 947-7396
www.nrcan.gc.ca/cfs/

To order publications on-line, visit the Canadian Forest Service Bookstore at:
bookstore.cfs.nrcan.gc.ca